J Am Soc Nephrol 11: 477–489, 2000

Effect of Angiotensin-Converting Enzyme Inhibition on Glomerular Basement Membrane Permeability and Distribution of Zonula Occludens-1 in MWF Rats

DANIELA MACCONI,* MARINA GHILARDI,* MARIA ENRICA BONASSI,* EHAB I. MOHAMED,* MAURO ABBATE,* FRANCESCA COLOMBI,* GIUSEPPE REMUZZI,*† and ANDREA REMUZZI*

**Department of Kidney Research, Mario Negri Institute for Pharmacological Research, and †Unit of Nephrology and Dialysis, Azienda Ospedaliera, Ospedali Riuniti di Bergamo, Bergamo, Italy.*

Abstract. The mechanism(s) by which angiotensin-converting enzyme (ACE) inhibitors prevent glomerular membrane loss of permselective function is still not understood. In male MWF rats, which develop spontaneous proteinuria with age, ACE inhibitors prevent proteinuria and increase glomerular ultrafiltration coefficient. These renoprotective effects are not associated with ultrastructural changes of capillary wall components. This study was undertaken to investigate whether ACE inhibitors modulate functional properties of glomerular basement membrane (GBM) and/or of epithelial cells, both of which have been suggested to play a role in the maintenance of the glomerular filtration barrier. The hydraulic and macromolecular permeability of the GBM were determined, by an *in vitro* filtration system, in untreated or lisinopril-treated rats and in Wistar rats taken as controls. By indirect immunofluorescence and immunoelectron microscopy, glomerular distribution of the tight junction protein zonula occludens-1 (ZO-1), a component of the slit diaphragm, was also studied. Results document that spontaneous proteinuria in MWF rats develops without significant changes in the permeability of the GBM to water and albumin, or in the ultrastructure of the podocyte foot processes, but is associated with an important alteration in the distribution of ZO-1 at the glomerular level. Lisinopril, which prevented proteinuria, also prevented glomerular redistribution of the protein. Thus, renoprotective effects of ACE inhibitors are not associated with changes in intrinsic functional properties of GBM, or ultrastructural changes of the epithelial cells, but rather with preservation of glomerular ZO-1 distribution and slit diaphragm function, which are essential for maintaining the filtration barrier.

Under normal circumstances, the glomerular capillary wall functions as an efficient and selective barrier that allows a high flow rate of filtration for plasma water and small solutes, but almost completely retains macromolecules the size of albumin or larger (1,2). Several experimental studies and clinical investigations in the past have focused on understanding how glomerular membrane permselective function is damaged or lost during development of proteinuric glomerular diseases. This is still an open question and is of crucial importance, because a growing body of evidence suggests that abnormal filtration of plasma proteins through the glomerular capillary wall has an intrinsic toxicity on the proximal tubule and subsequently on the whole kidney, and seems to represent a key factor in renal disease progression (3–6). Additional interest in this area has been generated by the observation that inhibition of angiotensin-converting enzyme (ACE) prevents or reduces urinary protein excretion, glomerular injury, and renal function deterioration in experimental animals (7–10) and in humans (11–15).

The experimental investigation of glomerular capillary wall permeability properties has suggested that in an experimental model characterized by massive proteinuria, such as passive Heymann nephritis, proteinuria depends on the recruitment of previously unexposed, large, nonselective pores, which constitute an escape pathway permeable to macromolecules (16). Studies by our group in male MWF rats, which develop spontaneous proteinuria with age (17,18), have shown that angiotensin II inhibition or antagonism prevented proteinuria by preserving size-selective function of the glomerular capillary (10,19). This effect of angiotensin II inhibition has also been demonstrated in human renal diseases (12,20–22). Using micropuncture technique, we have observed that in the MWF rat ACE inhibition is associated with increased glomerular ultrafiltration coefficient (K_f, the product of hydraulic permeability and the filtering surface area of glomerular membrane) (10). Morphometric studies in the same model indicated that this elevation of K_f induced by ACE inhibitors was not the consequence of increased glomerular filtering surface area (23), but

Received March 18, 1999. Accepted August 25, 1999.
Dr. Timothy Meyer served as Guest Editor and supervised the review and final disposition of this manuscript.
This study was presented in part at the 29th Annual Meeting of the American Society of Nephrology, November 3–6, 1996, New Orleans, LA, and at the 31st Annual Meeting of the American Society of Nephrology, October 25–28, 1998, Philadelphia, PA.
Correspondence to Dr. Daniela Macconi, "Mario Negri" Institute for Pharmacological Research, Via Gavazzeni, 11, 24125 Bergamo, Italy. Phone: +39 035 319 888; Fax: +39 035 319 331; E-mail: macconi@irfmn.mnegri.it
1046-6673/1103-0477
Journal of the American Society of Nephrology

must be attributed primarily to an elevation of the hydraulic permeability of the glomerular capillary wall. Structural and theoretical evidence suggests that the hydraulic resistance of the glomerular capillary wall is attributed half to the glomerular basement membrane (GBM) and half to the slit diaphragm of the epithelial podocytes, and we investigated in a previous study whether ACE inhibitor treatment modified GBM thickness and/or the epithelial podocyte ultrastructure in MWF rats. In that study, no changes were found in GBM thickness, configuration of epithelial podocytes, or in the width and frequency of the epithelial slit diaphragms between treated and untreated animals (23). Thus, maintenance of the glomerular filtration function induced by ACE inhibition does not derive from detectable ultrastructural changes of capillary wall components, but rather must derive from action on its intrinsic functional properties.

The aim of the present study was to address this issue in more depth. We first focused our attention on the GBM, which seems to play a role in determining, at least in part, both hydraulic and macromolecular permeability properties of the glomerular membrane (24,25). To evaluate the permeability properties of the GBM, independently from glomerular hemodynamics and glomerular cells, we used an *in vitro* filtration technique, based on water and macromolecule filtration across isolated glomerular membrane fragments consolidated under pressure to form a continuous film (26,27). We investigated whether permeability to water and albumin of reconstituted GBM is different in MWF rats compared with normal Wistar rats used as controls. We also studied whether the renoprotective effect of ACE inhibitors, observed *in vivo* in these animals, depends on the modulation of hydraulic and macromolecular permeability of the GBM.

More recent evidence suggests that glomerular epithelial cells, besides the GBM, also play an important role in maintaining the permselective function of the glomerular capillary wall and in particular that the slit diaphragms strongly influence water and protein filtration across the glomerular membrane (28–32). In line with these findings, it has been documented that experimental nephrosis is associated with a reorganization of the filtration slits and glomerular redistribution of the tight junction protein zonula occludens-1 (ZO-1), a component of the slit diaphragm, which seems to play a pivotal role in maintaining the permselective properties of the glomerular capillary wall (33). Thus, on the basis of the above observations, we investigated whether proteinuria, in male MWF rats, is associated with alterations of ZO-1 distribution within the glomerular membrane and/or changes in the ultrastructure of the epithelial foot processes, and whether ACE inhibition influences both parameters. Wistar rats were used as normal controls for these comparisons.

Materials and Methods

Study Design

Forty-five male MWF rats of 10 wk of age and 24 male Wistar rats were used for these studies. MWF rats were bred and raised in our facilities (17). Wistar rats were purchased from Charles River (Calco, Italy). All animals were allowed free access to food (standard rat chow containing 23% protein by weight) and water. For filtration experiments, three groups of animals were used. Twelve male Wistar rats weighing 350 to 420 g were used as normal controls (group 1); 11 male MWF rats received no therapy and were followed until the age of 25 to 30 wk (group 2); eight male MWF rats of 10 wk of age were given the ACE inhibitor lisinopril (Zeneca Pharmaceutical, Macclesfield, United Kingdom) at a dose of 40 mg/L in the drinking water for 15 to 18 wk (group 3). Before treatment and at the end of the observation period, systolic BP (SBP) was measured by tail plethysmography in awake animals, and urinary protein excretion was determined by 24-h urine collections and Coomassie blue G dye-binding assay as described previously (10). Filtration experiments were performed at the end of the observation or treatment period, the time at which we have previously shown that untreated rats are proteinuric but develop only minor changes of the glomerular structure (18). For the evaluation of glomerular distribution of ZO-1 and ultrastructural components of the glomerular capillary wall, three other groups of animals of 20 wk of age were used: 12 age-matched Wistar rats were used as normal controls (group 4), 15 MWF rats were left untreated (group 5), and 11 MWF rats were treated with the ACE inhibitor lisinopril from 10 to 20 wk of age (group 6). Experimental work and animal care procedures were conducted in accordance with the institutional guidelines outlined by national and international laws and policies (EEC Council Directive 86/609, OJ L 358-1, NIH Guide for the Care and Use of Laboratory Animals).

GBM Isolation

Rats of groups 1 to 3 were anesthetized with inactin (100 mg/kg, intraperitoneally), and both kidneys were perfused *in situ* at 120 mmHg with Tris-buffered saline (0.15 M NaCl, 0.05 M Tris(hydroxymethyl) aminomethane/HCl buffer, pH 7.4) until blanching. Kidneys were removed and weighed. All subsequent preparative steps were performed at 4°C. The renal capsules were dissected away, and the cortexes were separated from the medulla, weighed, and finely minced. The homogenate was sequentially pressed through 180- and 150-μm sieves, which excluded most of the tubules, and then washed with Tris-buffered saline, pH 7.4, with 0.1% Tween over a 75-μm sieve to retain glomeruli. The purity of the resulting preparation, consisting of intact decapsulated glomeruli, was determined microscopically and was higher than 90%.

The GBM was prepared by detergent lysis of isolated glomeruli with *N*-lauroyl-sarcosine as described previously (34). Briefly, *N*-lauroyl-sarcosine (0.5%, wt/vol, in Tris-buffered saline, 20 ml/g cortex) was added to the glomerular pellet and vigorously homogenized for 2 min. After standing for 10 min, the suspension was centrifuged at 2000 $\times$ *g* for 2 min and the sediment was resuspended in fresh detergent (4 ml/g cortex), vigorously shaken, and again centrifuged as above. The residue was washed once in Tris-buffered saline, suspended in unbuffered 0.15 M NaCl containing 0.01% (wt/vol) deoxyribonuclease 1 (1.5 ml/g cortex, Type DN 25; Sigma Chemical Co., St. Louis, MO), vortexed, and allowed to stand for 30 min at room temperature. The capillary "skeletons" were centrifuged, suspended in 4 ml of Krebs buffer (120 mM NaCl, 4.8 mM KCl, 1 mM KH_2PO_4, 1.2 mM $CaCl_2$, 0.6 mM $MgSO_4$, 24 mM $NaHCO_3$, 180 mg/dl glucose; pH adjusted to 7.4 before use), and sonicated. Membrane fragments were then used for filtration experiments. All solutions were filtered (0.22-μm pore size filters; Millipore, Bedford, MA) immediately before use to remove contaminants, and glassware were precoated with silicon (Sigmacote; Sigma Chemical Co.).

Filtration Experiments

For filtration experiments, an Amicon mini-ultrafiltration cell (model 3) was modified to include a sampling port connected by a three-way stopcock to a roller pump for periodic sampling of the retentate and buffer refilling. A Whatman 50 hardened filter paper and a HAWP 0.45-μm Millipore membrane were layered at the base of the ultrafiltration cell. GBM suspended in Krebs buffer, pH 7.4, was loaded into the cell, and pressure in the cell increased with N_2 gas to 1.5 atm for 1 h to form a continuous film of membrane fragments on the Millipore surface. Once GBM was consolidated, we examined the effect of transmembrane hydraulic pressure difference (ΔP) concentration on hydraulic permeability of the GBM in the absence of albumin. The buffer was filtered through the cell at the applied pressure of 50, 100, 200, and 300 mmHg. At each pressure level, after a 3-min equilibration period, 5 min of collection were carried out. Filtrate was collected in preweighed tubes to calculate water filtration rate. Buffer was then removed, and the cell was rinsed with retentate solution containing bovine serum albumin (BSA) (in Krebs buffer, pH 7.4) and then assembled with the magnetic stirrer. Filtration of albumin was first performed at ΔP of 300 mmHg (under continuous stirring at 220 rpm) for 20 min for equilibration. Then a collection period of 10 min was performed. Pressure was subsequently decreased to 200, 100, and 50 mmHg, and, for each pressure level, the clearance of albumin was determined preceded by a 10-min equilibration period. The retentate was sampled at the start and completion of the collection period, and the filtrate was collected throughout the 10-min clearance in preweighed tubes. The flux of water and albumin and the clearance and the fractional clearance of albumin were calculated. Albumin concentration was determined in both filtrate and retentate fractions by Coomassie blue G dye-binding assay (35). All of the experiments were performed at 25°C. At the end of each filtration experiment, the GBM-Millipore filter was perfused with buffer for 10 min at ΔP of 50 mmHg, fixed with glutaraldehyde 2.5% for 20 min at the same ΔP, and processed for light microscopy and morphometric evaluation of GBM layer. Light microscopic slides of the GBM-Millipore filter embedded with random orientation were stained with periodic acid-Schiff for determination of the thickness of GBM layers. In GBM layers obtained from animals of group 1, the effect of pH in the filtration fluid was studied. To this purpose, an identical procedure was used to evaluate the permeability properties of the GBM to water and albumin at pH 5.7 ($n = 5$) and 7.4 ($n = 7$).

Calculations

Volumetric flow (Q) was measured by collecting the filtrate during timed intervals in preweighed test tubes. Volume flux (J_v) was then calculated as:

$$J_v = \frac{Q}{A},$$

where A is the effective membrane surface area available for filtration (1.54 cm^2). Hydraulic permeability (L_p) of the reconstructed GBM layer was calculated as:

$$L_p = \frac{J_v}{\Delta P},$$

where ΔP is the hydraulic pressure difference across the filtration membrane. According to Daniels and coworkers (27), hydraulic permeability in presence of albumin ($L_{p_{alb}}$) was calculated taking into account the effect of transmembrane oncotic pressure of albumin ($\mathbf{\Delta\Pi}_{alb}$):

$$L_{p_{alb}} = \frac{J_v}{(\Delta P - \sigma_{alb}\Delta\Pi_{alb})},$$

where σ_{alb} is the albumin reflection coefficient. Assuming that albumin transport across the filter is mainly due to convection, the albumin reflection coefficient was calculated as:

$$\sigma_{alb} = 1 - \theta_{alb},$$

where θ_{alb} is the membrane sieving coefficient for albumin that is given by the ratio between the albumin concentrations at the two sides of the membrane. Thus,

$$L_{p_{alb}} = \frac{J_v}{(\Delta P - (1 - \theta_{alb})\Delta\Pi_{alb})},$$

where $\Delta\Pi_{alb}$ was calculated from C_{alb} using the Landis–Pappenheimer equation.

To take into account the concentration polarization effects of albumin at the surface of GBM, which increases albumin concentration near the GBM layer, we used the formulation proposed by Daniels and coworkers (27) for the calculation of the membrane θ_{alb} from the overall θ'_{alb}, the ratio between albumin concentration in the filtrate fluid over that in the retentate.

$$\theta_{alb} = \frac{\theta'_{alb}}{(1 - \theta'_{alb})B + \theta'_{alb}},$$

where the polarization coefficient B has the form:

$$B = \exp\left(\frac{J_v}{k_c}\right),$$

and k_c is a mass transfer coefficient assumed to be $k_c = 4.36 \times 10^{-4}$ cm/s, and is a function of albumin diffusivity, viscosity of the solution, and speed of rotation of the stirrer (27).

To estimate local hydraulic permeability properties of the extracellular matrix that composes GBM, we calculated the Darcy permeability (K_D) as:

$$K_D = L_p \times \mu \times \overline{\Delta x} \text{ or } K_{D_{alb}} = L_{p_{alb}} \times \mu_{alb} \times \overline{\Delta x},$$

respectively, in the absence or presence of albumin, where $\overline{\Delta x}$ is the thickness of the GBM layer, and μ and μ_{alb} are the dynamic viscosity of filtration solution without or with albumin, respectively. These viscosities were calculated from direct estimations of cinematic viscosity at room temperature using a glass viscometer.

Morphometry of GBM Layers

Thickness of GBM films used for filtration experiments (Δx) was determined by conventional morphometric technique of GBM-Millipore filter sections using a light microscope connected to a computer-based image analysis system as described previously (23). Briefly, images of the GBM layers were systematically acquired, randomly oriented, and digitally overlaid with a hortogonal grid (9 × 11 lines), and GBM layer thickness was measured in screen pixels over the grid lines intersecting the membrane in vertical and horizontal direction. A minimum of 500 measurements in both directions was made for each

filter. The mean thickness of GBM layers was then calculated using the harmonic mean $\overline{T_h}$ as described previously (23):

$$\overline{\Delta x} = \frac{8}{3\pi} \times \overline{T_h},$$

where $8/3\pi$ is a correction factor for variation in the angle of section through GBM.

Immunohistochemistry

For immunohistochemistry, the left kidney in each animal was flushed with Dulbecco's minimal essential medium through the abdominal aorta and fixed *in situ* by perfusion with aldehyde fixative (3% paraformaldehyde, 0.05% glutaraldehyde buffered with 0.1 M sodium phosphate buffer, pH 7.4) at room temperature. The kidney was then removed, cut along the midcoronal section, and immersed in the same fixative for an additional hour at 4°C. Thereafter, tissue specimens were immersed in 30% sucrose in phosphate-buffered saline (PBS) for at least 2 h at 4°C, embedded in OCT medium, and frozen in liquid nitrogen. Tissue sections (3 μm) were cut using a Mikrom cryostat (HM 500 O; Walldorf, Germany) and stored at −80°C until further processing.

Before ZO-1 staining, the structural integrity of tissue sections was checked by direct immunofluorescence with FITC-conjugated wheat germ agglutinin (12.5 μg/ml in PBS; Vector Laboratories, Burlingame, CA). ZO-1 was detected with the affinity purified-rabbit anti-ZO-1 (10 μg/ml in PBS; Zymed Laboratories, South San Francisco, CA) overnight at 4°C, followed by three 5-min washes with PBS at room temperature and by incubation with Cy3-conjugated goat anti-rabbit IgG antibodies (affinity-purified, 7.5 μg/ml in PBS; Jackson ImmunoResearch Laboratories, West Grove, PA) for 1 h at room temperature. For each section, nonspecific binding of antibodies was blocked with PBS/1% BSA. After final washing with PBS, slides were mounted using 100 mM Tris HCl:glycerol (50:50), 2% *N*-propyl gallate, pH 8.0. Sections were examined with a light microscope (BH2; Olympus Optical Co., Tokyo, Japan) equipped with epifluorescence and appropriate filters. In each section, the glomerular distribution of immunofluorescence staining for ZO-1 was classified as previously reported (33). A score was assigned to each individual glomerulus in the section tissue. The scores 0, 0.5, and 1.0 were used, respectively, for: continuous distribution along the glomerular capillary wall; heterogeneous distribution of ZO-1 along the glomerular membrane, with staining intensity variable from one region to another within the same glomerulus; and markedly discontinuous distribution of ZO-1. The final score ($DS_{ZO\text{-}1}$) per section was then calculated as the weighted mean:

$$DS_{ZO\text{-}1} = \frac{(N_1 \times 0 + N_2 \times 0.5 + N_3 \times 1)}{(N_1 + N_2 + N_3)},$$

where N_i ($i = 1$ to 3) is the number of glomeruli in each category. The scores were assigned by two observers, blinded to the nature of the experimental groups, and the mean of the two estimations was calculated. More than 80 glomeruli on average per section were evaluated by each observer. As negative control, incubation of the sections with the secondary antibody alone was performed and resulted in a complete prevention of staining at the glomerular level.

Immunoelectron Microscopy

Three animals of groups 4, 5, and 6 were used for immunogold studies and Western blot analysis. For immunogold staining, the left kidney was flushed with PBS through the abdominal aorta and fixed *in situ* by perfusion with paraformaldehyde-lysine-periodate fixative (2% paraformaldehyde, 0.075 M lysine, 0.01 M sodium periodate in 0.0375 M sodium phosphate buffer) at room temperature (36). The kidney was then removed, cut along the midcoronal section, and immersed in the same fixative overnight at 4°C. Thereafter, fragments of periodate-lysine paraformaldehyde-fixed kidneys were infiltrated with 2.3 M sucrose for 1 h and sectioned at approximately −100°C, using a Reichert fetal calf serum ultracryomicrotome (37). Ultrathin sections were transferred to nickel grids (200 mesh) coated with Formvar and stored at 4°C on 1% gelatin until use. After quenching free aldehyde groups with 10% fetal calf serum containing 0.01 M glycine, sections were incubated overnight (4°C) with the affinity-purified rabbit anti-ZO-1 (10 μg/ml in PBS/1% BSA) followed by 1 h incubation at room temperature with 10-nm gold-conjugated goat anti-rabbit IgG (1:50, in PBS/1% BSA, Sigma Chemical Co.). After incubation, the grids were washed once with high-salt PBS and twice with PBS, fixed for 10 min in 1% glutaraldehyde, washed again in distilled water, and stained for 5 min with 2% aqueous uranyl acetate. Grids were then destained and embedded in methylcellulose before examining with a Zeiss EM 109 electron microscope (Carl Zeiss, Oberkochen, Germany).

Western Blot Analysis

The right kidney of the above animals was perfused with ice-cold PBS containing protease inhibitors (1 mM each benzamidine, phenylmethylsulfonyl fluoride, 10 μg/ml each leupeptin, antipain, pepstatin A, and 5 mM EDTA), after which isolated glomeruli were obtained by differential sieving as described above. All isolation steps were performed at 4°C in the presence of protease inhibitors. The glomerular pellet was solubilized in SDS-PAGE sample buffer (2% SDS, 10% glycerol, 0.08 M (hydroxymethyl)aminomethane (Tris) hydrochloride, pH 6.8) without bromphenol blue and centrifuged at 14,000 × *g* for 5 min to remove insoluble material. The protein concentration was measured by Lowry. Forty micrograms of protein per lane were electrophoresed under reducing conditions on 5% polyacrylamide slab gels (0.75 mm thick) (38) and transferred to nitrocellulose membranes (39). The membranes were incubated 1 h at room temperature with blocking buffer (5% skim milk, 0.2% Tween in PBS) followed by overnight incubation at 4°C with rabbit anti-ZO-1 (1:1000 in 3% skim milk, 0.1% Tween in PBS). The bound IgG was detected by incubation for 1 h at room temperature with alkaline phosphatase-conjugated goat anti-rabbit IgG $F(ab')_2$ fragments (1:5000 in 3% skim milk, 0.1% Tween in PBS) followed by Fast Red (Boehringer Mannheim).

Electron Microscopy

After *in situ* fixation, the right kidney was removed and cut in small pieces (1 mm^3), which were immersed in 2.5% glutaraldehyde buffered with 0.1 M sodium cacodylate buffer, pH 7.4, for 4 h at room temperature, washed in cacodylate buffer, and then post-fixed with 1% OsO_4 for an additional hour. Fixed specimens were dehydrated with graded concentrations of ethanol and embedded in Epon resin. Ultrathin sections (100 nm) were cut on an ultramicrotome (LKB 2088 UltrotomeV; LKB-Produkter, Bromma, Sweden), collected on Formvar-coated slot grids, and stained with uranyl acetate and lead citrate. Ultrastructural evaluations were done by a pathologist blinded to the nature of the study, using a Zeiss EM 109 electron microscope.

Evaluation of Glomerular Epithelial Ultrastructural Changes

Epithelial foot process width (W_{FP}) was measured according to previously described methods (23,40), using computer-based mor-

phometry. Briefly, eight photomicrographs were systematically obtained from two to three glomerular cross-sections per animal using electron microscopy. Photomicrographs were printed at a final magnification of ×12,800, and a calibration grid with 2160 lines/mm (Fullam, Inc., Schenectady, NY) was used to monitor exact magnification. The micrographs were then digitized using a flat scanner and transferred to the computer-based morphometric system. The mean width of the podocyte foot processes ($\overline{W}_{FP}$) was calculated as the harmonic mean (23,41):

$$\overline{W}_{FP} = \frac{8}{3\pi} \times \frac{N}{\sum_i \frac{1}{W_i}},$$

where N is the number of foot processes measured and W_i is the length of the segments connecting the center line of two adjacent filtration slits, measured using image processing software (NIH Image version 1.60) with final magnification on the computer screen of ×36,000. The harmonic mean takes into account that epithelial foot processes are sectioned with random orientation. More than 500 foot processes were measured in each glomerulus.

Statistical Analyses

All results are expressed as mean ± SD. Data were analyzed by one-way ANOVA, and differences between individual group means were assessed by Tukey–Cicchetti test for multiple comparisons (42). Scores for glomerular distribution of ZO-1 along the glomerular capillary wall by indirect immunofluorescence in the three groups were compared with the Kruskal–Wallis test for nonparametric data. Statistical significance was defined as $P < 0.05$.

Results

Mean SBP and urinary protein excretion of rats used for filtration experiments performed at pH 7.4 are reported in Figure 1. As expected (10), SBP was elevated in untreated MWF rats (group 2) of 25 to 30 wk of age above the mean value measured in control Wistar rats (group 1) (Figure 1, top panel). Proteinuria developed spontaneously with age in untreated MWF rats (group 2), increasing from 68 ± 16 mg/d (basal value) to 276 ± 131 mg/d at 25 to 30 wk of age (Figure 1, bottom panel). ACE inhibition with lisinopril, besides controlling BP, significantly prevented the increase in urinary protein excretion (Figure 1). Body weight was comparable in these three groups of rats, whereas kidney weight was significantly lower in lisinopril-treated rats compared to untreated MWF (1.23 ± 0.08 *versus* 1.41 ± 0.17 g, $P < 0.05$) and Wistar rats (1.49 ± 0.16 g, $P < 0.01$).

The permeability properties of GBM to water and albumin at pH 7.4 were evaluated using the *in vitro* filtration technique at transmembrane hydraulic pressure difference (ΔP) ranging from 50 to 300 mmHg. From water and albumin filtration rate at each ΔP level, and measured mean thickness of GBM layers Δx, the Darcy permeability (K_D) was calculated. As shown in Table 1, K_D, either in the absence or presence of albumin, was comparable between untreated MWF and Wistar rats. Furthermore, treatment of MWF rats with lisinopril for about 18 wk did not affect significantly the hydraulic permeability of GBM. Albumin permeability of GBM in proteinuric MWF rats calculated as albumin clearance corrected for concentration polarization effect (θ_{alb}) was comparable to that measured in GBM from Wistar animals taken as normal controls (Table 2). Lisinopril effectively prevented proteinuria in MWF rats, but did not affect albumin permeability through the GBM at the statistically significant extent (Table 2). As shown by the results reported in Table 3, albumin permeability (θ_{alb}) of GBM in Wistar rats was comparable at pH 7.4 and pH 5.7, indicating that electric charge did not affect the filtration behavior of albumin.

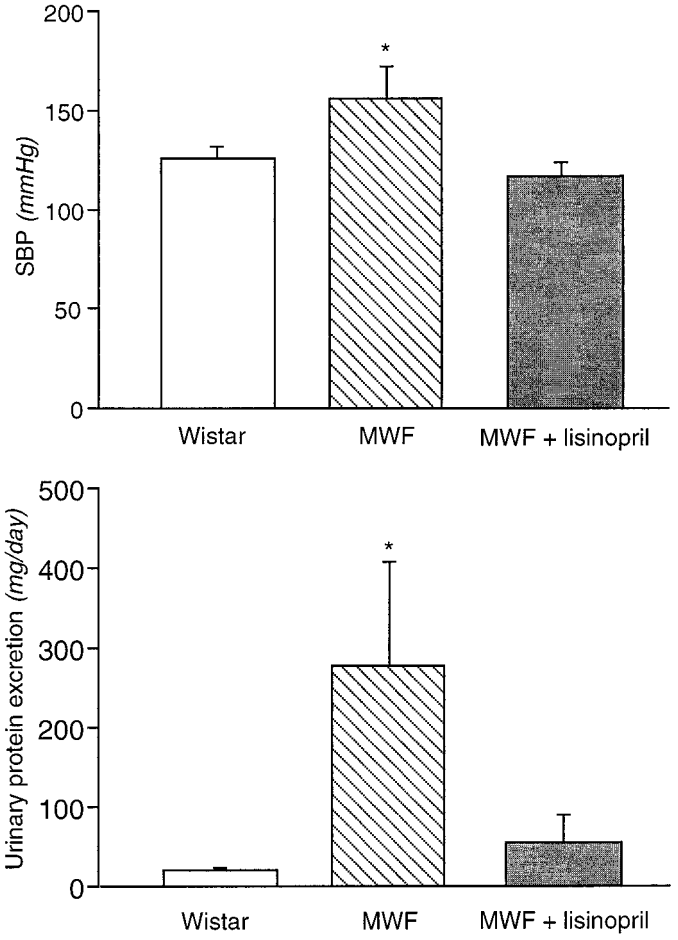

Figure 1. Systolic BP (SBP) and urinary protein excretion in Wistar rats ($n = 7$) and in untreated ($n = 12$) or lisinopril-treated ($n = 8$) MWF rats at the end of the observation period or treatment. Results are mean ± SD. *$P < 0.01$ *versus* Wistar rats and *versus* lisinopril-treated MWF rats.

The results on glomerular ZO-1 distribution are reported in Figures 2 and 3. In normal kidneys from Wistar rats (group 4), the immunofluorescence labeling for ZO-1 was uniformly distributed along the peripheral capillary loop in almost the entire number of glomeruli examined (Figure 2, A and B). An average score of 0.22 ± 0.20 was calculated for glomerular ZO-1 distribution (Figure 3). The pattern of glomerular staining of ZO-1 was markedly different in proteinuric MWF rats (group 5), appearing more heterogeneous and discontinuous (Figure 2, C and D). The score of ZO-1 distribution averaged 0.58 ± 0.24 in this group, a value significantly higher than that computed

Table 1. Darcy permeability of GBM layers in the absence (K_D) or presence of albumin ($K_{D_{alb}}$)[a]

ΔP (mmHg)	K_D (nm^2)			$K_{D_{alb}}$ (nm^2)		
	Wistar ($n = 7$)	MWF ($n = 11$)	MWF + Lisinopril ($n = 8$)	Wistar ($n = 7$)	MWF ($n = 11$)	MWF + Lisinopril ($n = 8$)
50	1.76 ± 0.43	1.46 ± 0.49	1.74 ± 0.63	1.08 ± 0.16	1.09 ± 0.31	0.93 ± 0.38
100	1.37 ± 0.35	1.13 ± 0.55	1.53 ± 0.70	0.58 ± 0.10[b]	0.58 ± 0.21[b]	0.54 ± 0.12[b]
200	1.04 ± 0.27	0.86 ± 0.42	1.05 ± 0.39	0.33 ± 0.06[b]	0.33 ± 0.08[b]	0.30 ± 0.07[b]
300	0.85 ± 0.21[b]	0.71 ± 0.35[b]	0.87 ± 0.33[b]	0.23 ± 0.04[b,c]	0.25 ± 0.08[b,c]	0.21 ± 0.05[b,c]
$\overline{\Delta x}$ (μm)	7 ± 2	7 ± 2	6 ± 1	7 ± 2	7 ± 2	6 ± 1

[a] Results are mean ± SD. GBM, glomerular basement membrane; ΔP, transmembrane hydraulic pressure difference; $\overline{\Delta x}$, mean thickness of GBM layers.
[b] $P < 0.01$ *versus* same group at $\Delta P = 50$ mmHg.
[c] $P < 0.01$ *versus* same group at $\Delta P = 100$ mmHg.

Table 2. Permeability properties of GBM to albumin[a]

ΔP (mmHg)	θ_{alb}		
	Wistar ($n = 7$)	MWF ($n = 11$)	MWF + Lisinopril ($n = 8$)
50	0.20 ± 0.05	0.19 ± 0.08	0.22 ± 0.04
100	0.17 ± 0.03	0.17 ± 0.07	0.18 ± 0.04
200	0.15 ± 0.03	0.14 ± 0.06	0.16 ± 0.05
300	0.15 ± 0.04	0.12 ± 0.03	0.18 ± 0.06

[a] Results are mean ± SD. θ_{alb}, albumin clearance corrected for concentration polarization effect. Other abbreviations as in Table 1.

Table 3. Effect of pH on albumin permeability of GBM from Wistar rats[a]

ΔP (mmHg)	θ_{alb}	
	pH 7.4 ($n = 7$)	pH 5.7 ($n = 5$)
50	0.20 ± 0.05	0.19 ± 0.01
100	0.17 ± 0.03	0.15 ± 0.02
200	0.15 ± 0.03	0.13 ± 0.02
300	0.15 ± 0.04	0.13 ± 0.03

[a] Results are mean ± SD. Abbreviations as in Tables 1 and 2.

for group 4 ($P < 0.01$) (Figure 3). These changes in ZO-1 distribution cannot be attributed to structural changes of the glomerular tuft, since we measured that focal areas of glomerulosclerotic changes affected on average only 4% of glomerular population in untreated MWF rats.

The glomerular distribution of ZO-1 was also examined at the ultrastructural level by immunoelectron microscopy (Figure 4). In Wistar rats, immunogold labeling for ZO-1 localized almost exclusively on the cytoplasmic face of the podocyte plasma membrane near the point of insertion of the slit diaphragm (Figure 4A). In proteinuric MWF rats, immunogold labeling for ZO-1 was observed in the same region. In addition, frequent clusters of gold particles concentrated along the cytoplasmic side of the podocyte plasma membrane were also observed, suggesting a greater level of labeling of ZO-1 in these animals. Moreover, labeling for ZO-1 was also observed within the cytoplasm of podocyte foot processes (Figure 4, B and C). Such a localization of ZO-1 is in line with the altered distribution of the protein we found by immunofluorescence in MWF compared with Wistar rats. We also investigated whether glomerular expression of ZO-1 protein was different in Wistar and MWF rats. Western blot analysis of ZO-1 in glomerular lysate showed a comparable expression of the protein between the two groups (Figure 5). This finding suggests that proteinuria in MWF rats was associated with a redistribution of ZO-1 at the glomerular level rather than with changes in the amount of protein present.

Despite the development of proteinuria, and the important alteration of ZO-1 distribution, morphologic observation of glomerular membrane ultrastructure at the electron microscopy level did not show evident differences between untreated MWF animals and Wistar controls. No signs of abnormality were observed in GBM, podocyte foot processes, and filtration slits, except for small focal areas of epithelial cell effacement, which were observed to a similar extent in Wistar rats. Figure 6 shows representative micrographs of glomerular membrane at high-power electron microscopy in a normal Wistar rat and in a proteinuric MWF rat. Quantification of epithelial foot process width (W_{FP}) with morphometric analysis confirmed qualitative observation. As shown in Figure 7, a slight but not statistically significant difference was found between the two rat strains. Actually, $\overline{W}_{FP}$ averaged 306 ± 19 nm in the control Wistar group and 350 ± 28 nm in untreated MWF rats.

Treatment with lisinopril completely prevented proteinuria in MWF rats of group 6, compared with untreated MWF rats of group 5 (urinary protein excretion averaged 35 ± 14 and 233 ± 63 mg/d, respectively, in the two groups). The antiproteinuric effect of lisinopril was associated with important prevention of the alteration in glomerular distribution of ZO-1. As shown in Figure 2, E and F, the distribution of ZO-1 was markedly different from untreated MWF and more similar to Wistar animals. Indeed, the majority of glomeruli from lisino-

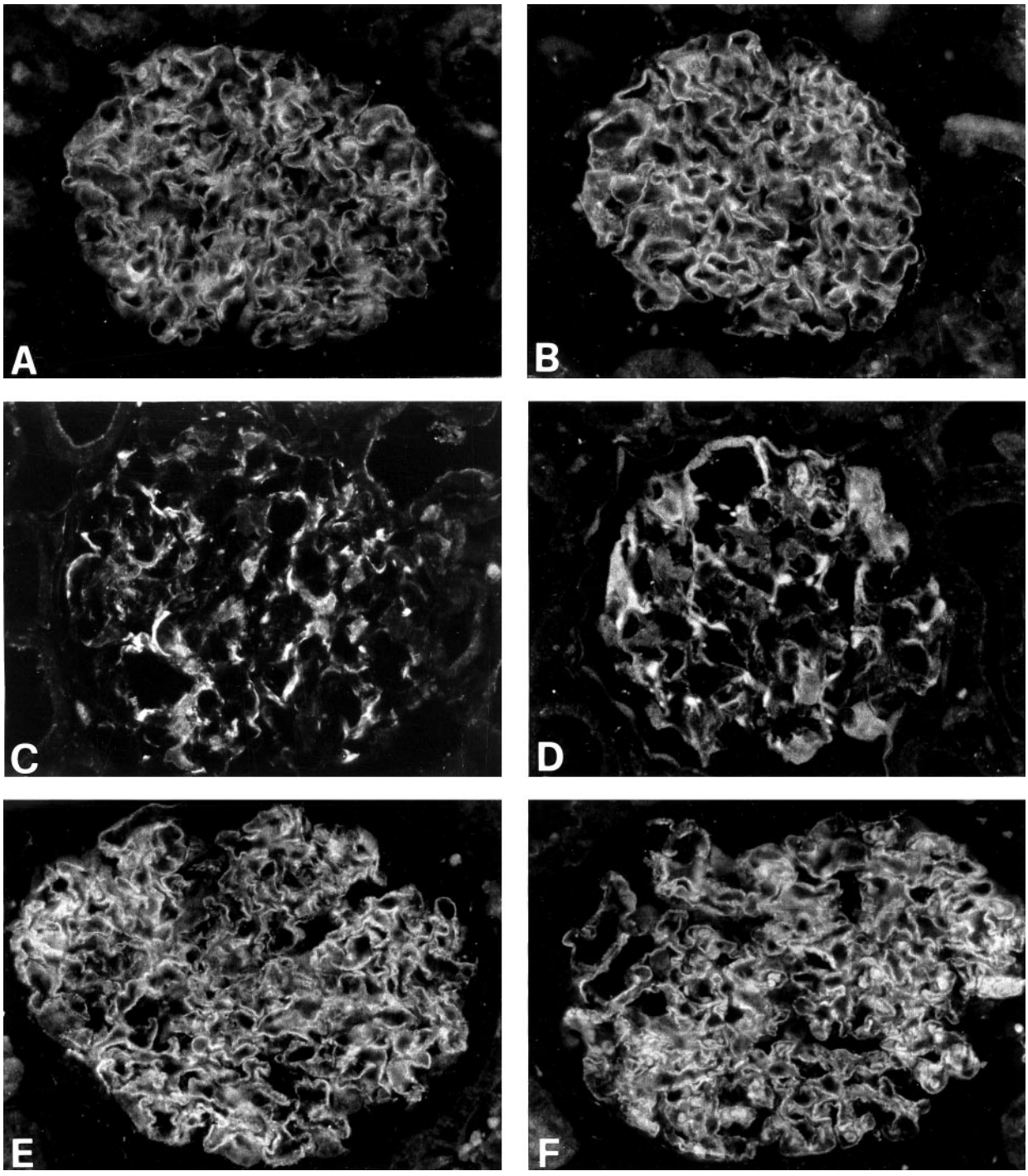

Figure 2. Representative immunofluorescence micrographs showing the distribution of zonula occludens-1 (ZO-1) in glomeruli from Wistar rats (A and B) and from untreated (C and D) or lisinopril-treated MWF rats (E and F).

pril-treated rats showed a continuous distribution of the protein along the glomerular membrane, comparable to the pattern observed in normal kidneys of Wistar rats (group 4), and the average score for ZO-1 distribution was 0.18 ± 0.07 ($P < 0.01$ *versus* untreated MWF rats) (Figure 3). Results of immunofluorescence were confirmed at the ultrastructural level (Figure 4). Immunogold labeling for ZO-1 in ultrathin cryosections of lisinopril-treated MWF rats revealed gold particles almost exclusively on the cytoplasmic side of the podocyte plasma membrane, as found in control Wistar rats, without clusters of gold particles and cytoplasmic labeling as observed in untreated MWF rats. As expected, ACE inhibition did not affect the expression of the protein in glomerular lysate, as shown in Figure 5.

The ultrastructure of the epithelial foot process in these animals was comparable to untreated MWF rats and to the

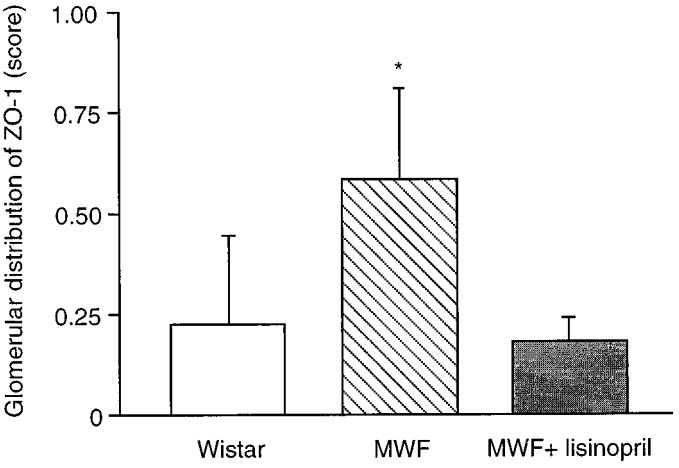

Figure 3. Score of the distribution of ZO-1 in glomeruli from Wistar rats and from untreated or lisinopril-treated MWF rats. Details about the score definition are given in Materials and Methods. Results are mean ± SD. $*P < 0.01$ *versus* Wistar rats and *versus* lisinopril-treated MWF rats.

Wistar rats (Figure 6). In particular, as for the other two groups, no signs of abnormality were observed in GBM and podocyte foot processes. The occasional focal areas of effacement in lisinopril-treated rats were comparable to the other two groups. Regarding changes in foot process dimensions, average $\overline{W}_{FP}$ by morphometric analysis was 317 ± 36 nm in lisinopril-treated animals, a value that is only numerically lower than that observed in untreated MWF animals, but the difference did not reach statistical significance (Figure 7).

Discussion

Under physiologic conditions, the small amount of albumin and larger plasma proteins filtered across the glomerular membrane are entirely reabsorbed at the tubular level. In pathologic conditions, an increased amount of plasma proteins, mainly albumin, is filtered across the glomerular capillary wall and is not completely reabsorbed at the tubular level, resulting in the so-called proteinuria of glomerular origin (43). It has been suggested that loss of size- as well charge-selectivity of the glomerular capillary wall are the functional alterations that lead to increased traffic of plasma proteins through the glomerular membrane. Ultrastructure and biochemical composition of the membrane would suggest that the GBM and epithelial layer both potentially exert size- and charge-selectivity functions (44). However, direct evidence of the precise mechanisms by which functional alterations of these layers of the capillary wall lead to proteinuria is still lacking.

We have used a spontaneous model of proteinuria in the male MWF rat to investigate possible functional and structural changes of individual components of the glomerular capillary wall that develop in these animals with age, as compared to the normal Wistar rat taken as control. In addition, because it has been demonstrated on several occasions that treatment of male MWF rats with ACE inhibitors prevents proteinuria (10,45), we investigated whether functional and structural changes of the glomerular capillary wall components are affected by this treatment. In a previous study (23) we reported that ACE inhibition, despite improving glomerular size-selective func-

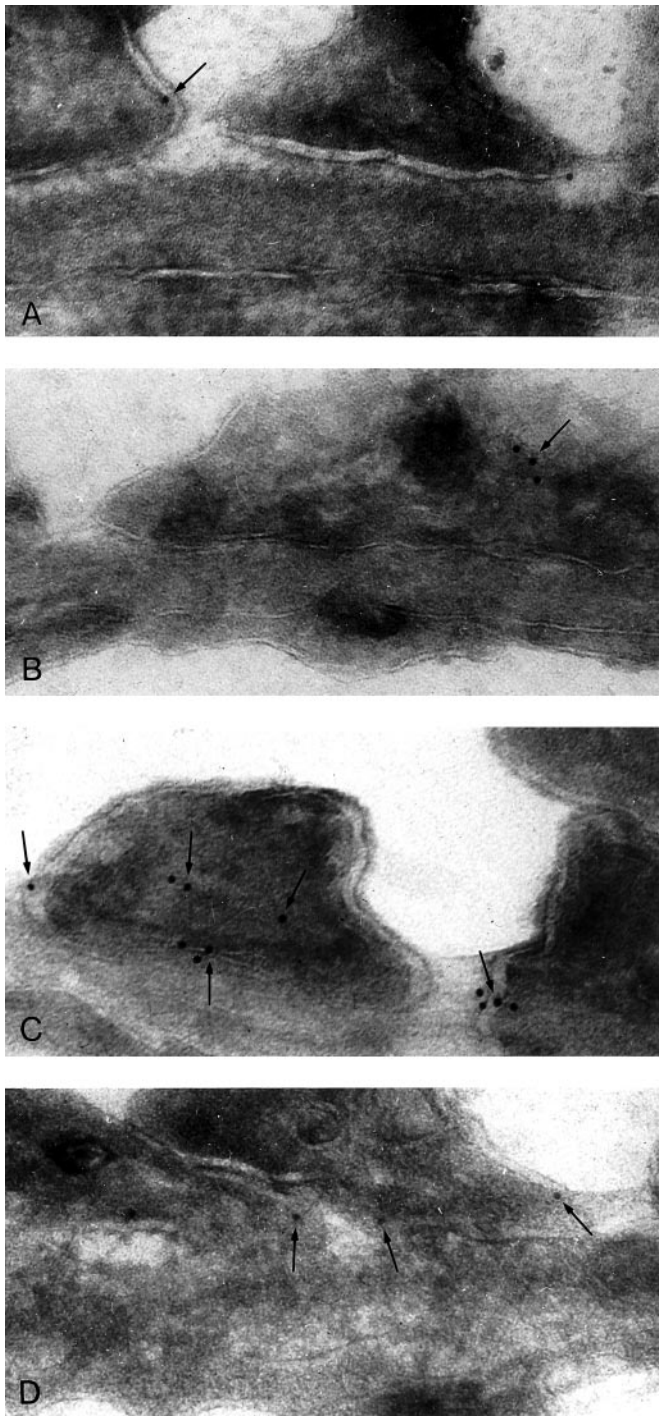

Figure 4. Representative pattern of immunogold labeling for ZO-1 in glomeruli from Wistar rats (A), and from untreated (B and C) or lisinopril-treated MWF rats (D). Gold particles (arrows) are localized on the cytoplasmic side of the podocyte plasma membrane at the point of insertion of the slit diaphragms (A and D). In proteinuric animals, clusters of gold particles are frequent both near the podocyte plasma membrane and within the cytoplasm of the podocyte foot processes (B and C). Magnification, ×30,000.

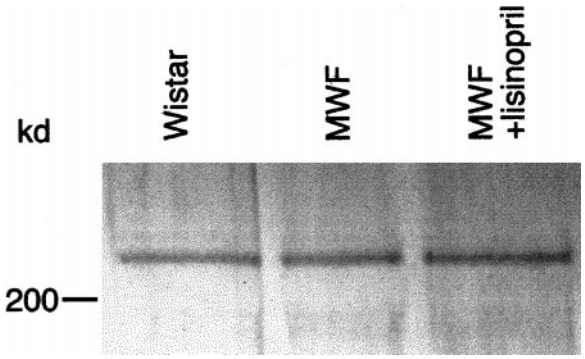

Figure 5. Representative Western blot analysis of glomerular lysate from Wistar rats and from untreated or lisinopril-treated MWF rats. For details, see Materials and Methods.

tion in male MWF rats (10), did not affect ultrastructure of the membrane components as observed by quantitative morphometric analysis, or the glomerular capillary surface area available for filtration.

On the basis of the above observation, here we first investigated whether development of proteinuria might depend on changes in permeability properties of the GBM to water and albumin. The results of our *in vitro* evaluations document that permeability properties of the GBM to water and albumin are comparable in proteinuric MWF rats and in normal Wistar rats—both K_D and θ_{alb} were not significantly different in the two groups—suggesting that functional alterations of GBM cannot explain the permselectivity defect of the glomerular membrane in proteinuric animals. In line with this result, ACE inhibition did not affect significantly the hydraulic permeability of GBM matrix and albumin filtration.

The maintenance of the GBM filtration barrier depends on the charge and size-based selectivity toward filtered macromolecules. In our system, in line with previous reports by Robinson and Walton (46), the electrostatic charge did not affect the behavior of albumin filtration through the GBM layer reconstructed from normal rats, indicating that size rather than charge is more prominent for restricting albumin passage through the GBM in normal circumstances. Very recently, Bolton and coworkers have elegantly documented that the sieving coefficients of Ficoll sulfate, in an *in vitro* filtration system, were not different from those of neutral Ficoll at physiologic ionic strength, but reduced at low ionic strength, suggesting that density of fixed negative charges of GBM is insufficient to confer significant charge selectivity under physiologic conditions (47). All of the above evidence supports the concept that the charge selectivity of the glomerular capillary wall does not depend on the GBM. Our present filtration study showing that alterations in GBM permeability to water and macromolecules do not develop in proteinuric MWF rats, and ACE inhibition does not change permeability properties of the GBM layer, strongly suggests that structural and/or functional changes of other components of the glomerular membrane must be responsible for glomerular permselectivity defect.

Several recent reports indicate that glomerular epithelial cells play a major role in water and protein permeability of the glomerular capillary wall (28–32). We then investigated the distribution of a tight junction component, the ZO-1 protein, which seems to play a crucial role in maintaining functional properties of the epithelial slit diaphragms (48–50), and morphologically evaluated the ultrastructure of the epithelial cell foot processes in the three experimental conditions adopted. Our present immunohistochemistry study documents that in normal Wistar rats, ZO-1 is uniformly distributed along the outer surface of the filtering membrane, whereas this pattern is markedly altered in proteinuric MWF rats, with a predominant discontinuous distribution of the ZO-1, with aggregation in focal points within the glomerular membrane (Figure 2). At the immunoelectron microscopy level, ZO-1 protein appears to be located not only at the cytoplasmic side of podocyte membrane, near the filtration slit, but also is present within the cytoplasm of the foot processes. The reason for the observed cytoplasmic labeling of the protein is behind the objective of our work, but it is suggestive of possible alteration in transport or compartmentalization of the protein within the podocytes. Independently of its origin, the abnormal protein distribution observed at electron microscopy level correlates with the abnormalities in the distribution observed in the immunofluorescence study in untreated MWF rats. Of interest, our Western blot analysis did not demonstrate changes in ZO-1 expression at the glomerular level, suggesting that the pattern observed at immunofluorescence derives mainly from a redistribution of the protein rather than from changes in its expression.

The redistribution of ZO-1 both at the optical and electron microscopy level that we have observed in proteinuric MWF rats has already been documented in experimental nephrosis induced in rats by puromycin aminonucleoside and in normal rat kidney perfused by the polycation protamine sulfate (33). In both cases, ZO-1 redistribution was associated with changes in the foot process ultrastructure and apical displacement of the glomerular slit diaphragm above the newly formed intercellular occluding-type junctions (33). At variance, in our model of spontaneous glomerular injury, the altered glomerular distribution of ZO-1 was not associated with any apparent ultrastructural change of the foot processes and the epithelial slit diaphragms on electron microscopy. More detailed investigation of the ultrastructure of the podocytes did not show a statistically significant difference in mean foot process width that was only numerically different in proteinuric animals compared with normal controls, as measured by morphometric technique. However, the qualitative and quantitative observations that we have obtained on electron microscopy are in line with a recent study by Kawachi and coworkers showing altered immunoreactivity of ZO-1 in glomeruli from rats injected with monoclonal antibody 5-1-6, which recognizes a 51-kD protein on the slit diaphragm and causes severe proteinuria, but does not induce changes in the structural integrity of the slit diaphragms (51). Of note, other conditions that induce abnormal urinary protein excretion, such as elevation of intrarenal angiotensin II (52) and reactive oxygen metabolites (53), appear not to be associated with changes in epithelial foot processes ultrastructure. On the other hand, in line with the present results, we have previously reported that prevention of proteinuria by ACE

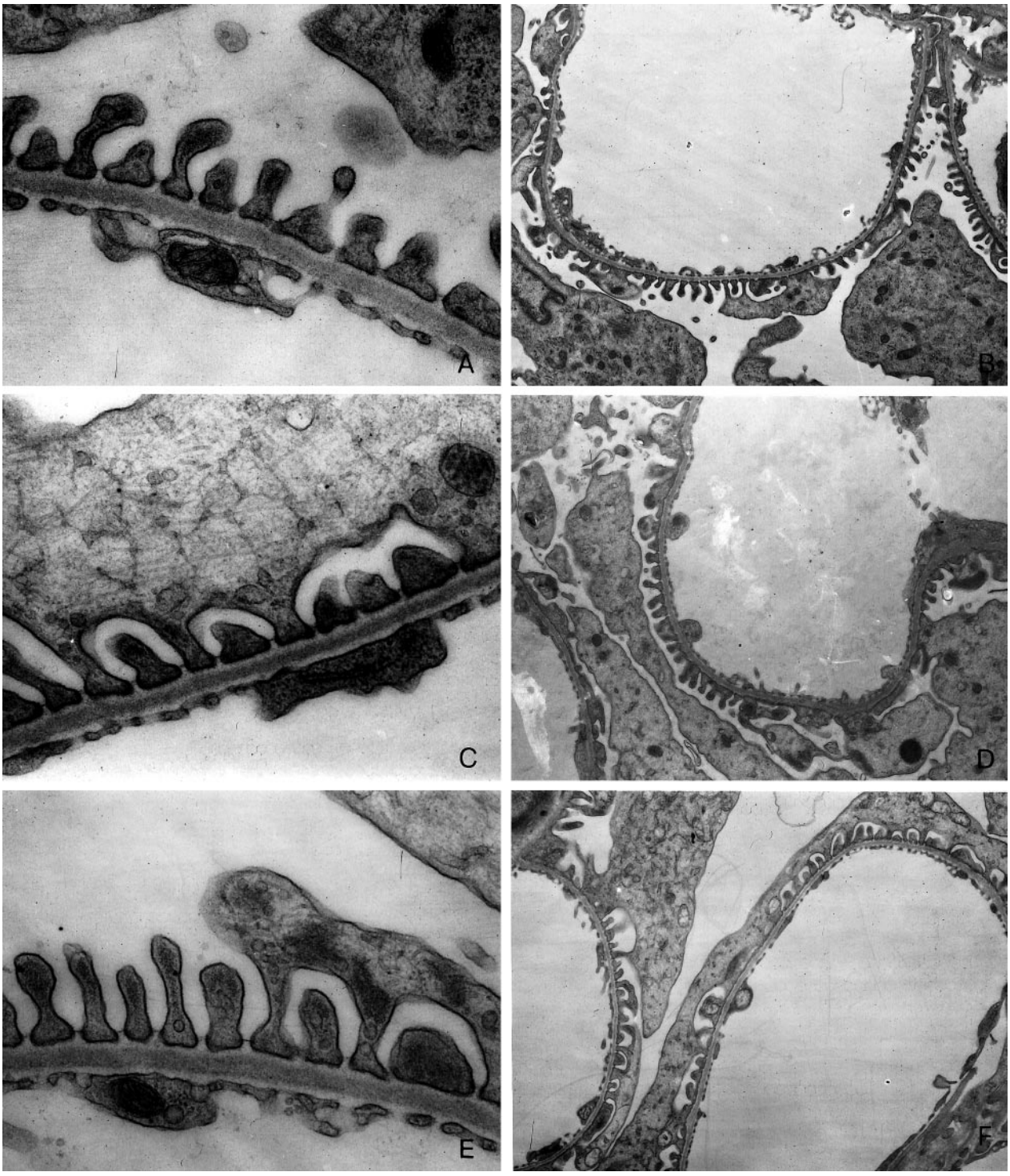

Figure 6. Transmission electron micrographs of representative glomeruli from Wistar rats (A and B) and from untreated (C and D) or lisinopril-treated MWF rats (E and F). Structural integrity of the slit diaphragms is maintained in proteinuric MWF rats. Magnification: ×29,400 in A, C, and E; ×4400 in B, D, and F.

inhibition in MWF rats was not associated with epithelial ultrastructural changes (23). Along this line, a human study (41) aimed at evaluating the relationship between glomerular foot process width and proteinuria in patients with glomerulonephritis has already documented that severe proteinuria can develop in the absence of ultrastructural changes of the foot processes, suggesting that foot process fusion is not a prerequisite for proteinuria.

Our present results further strengthen the concept that a molecular rather than a structural impairment must be responsible for abnormal glomerular filtration of plasma proteins. In addition, our findings that ACE inhibition, which is known to

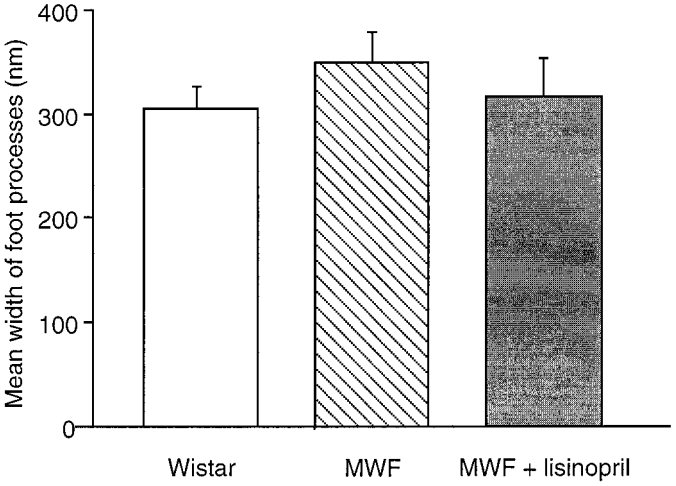

Figure 7. Mean foot process width in Wistar rats and in untreated or lisinopril-treated MWF rats. Results are mean ± SD.

prevent proteinuria and increase K_f (10), also prevented alteration in the glomerular distribution of ZO-1 both at the optical and electron microscopy level, strongly suggest that preservation of glomerular distribution of this protein and probably of some other not yet identified component of the slit diaphragm is essential for the maintenance of hydraulic permeability and permselective properties of the glomerular capillary wall. The mechanisms by which ZO-1 is redistributed and aggregated within the glomerular capillary wall in proteinuric conditions are behind the scope of the present study and are presently under investigation in our laboratory.

Altered distribution of ZO-1 has been documented in cultured podocytes exposed *in vitro* to cytokines, which cause a decrease in transmonolayer electrical resistance (54). It has been suggested that increased tyrosine phosphorylation of proteins at cell-cell junctions including ZO-1 protein may be responsible for the reorganization of the junctional complex and increase in paracellular permeability (55,56). ZO-1 has also been found to be phosphorylated in the tyrosine residues during rapid rearrangement of the glomerular filtration slits in experimental nephrosis (57). Finally, angiotensin II has been shown to induce tyrosine phosphorylation of proteins such as paxillin and PLCγ (58,59). On the basis of this evidence, it is tempting to speculate that angiotensin II causes a biochemical modification of ZO-1 in proteinuric MWF rats that may be responsible for impairment of the filtration slit diaphragm function and consequently of the filtration barrier.

In conclusion, our present investigations indicate that: (*1*) development of proteinuria in male MWF rats takes place without significant changes in GBM hydraulic and permselective function, or with changes in glomerular epithelial cell ultrastructure; (*2*) proteinuria in this model is associated with important alterations in glomerular distribution of the junction protein ZO-1; and (*3*) the antiproteinuric effect of ACE inhibitors is associated with preservation of glomerular ZO-1 distribution.

Acknowledgments

The authors thank Dr. Tullio Bertani for morphologic evaluation of glomerular membrane ultrastructure at electron microscopy level and Dr. Marina Morigi and Dr. Anna Fassi for helpful discussion.

References

1. Galaske R, Baladamus CA, Stolte H: Plasma protein handling in the rat kidney: Micropuncture experiments in the acute heterologous phase of anti-GBM-nephritis. *Pflügers Arch* 375: 269–277, 1978
2. Tojo A, Hitoshi E: Intrarenal handling of proteins in rats using fractional micropuncture technique. *Am J Physiol* 263: F601–F606, 1992
3. Remuzzi G: Abnormal protein traffic through the glomerular barrier induces proximal tubular cell dysfunction and causes renal injury. *Curr Opin Nephrol Hypertens* 4: 339–342, 1995
4. Remuzzi G, Bertani T: Is glomerulosclerosis a consequence of altered glomerular permeability to macromolecules? *Kidney Int* 38: 384–394, 1990
5. Hirschberg R: Bioactivity of glomerular ultrafiltrate during heavy proteinuria may contribute to renal tubulo-interstitial lesions. *J Clin Invest* 98: 116–124, 1996
6. Eddy AA: Experimental insights into the tubulointerstitial disease accompanying primary glomerular lesions. *J Am Soc Nephrol* 5: 1273–1278, 1994
7. Anderson S, Meyer TW, Rennke HG, Brenner BM: Control of glomerular hypertension limits glomerular injury in rats with reduced renal mass. *J Clin Invest* 76: 612–619, 1985
8. Zatz R, Dunn BR, Meyer TW, Anderson S, Rennke HG, Brenner BM: Prevention of diabetic glomerulopathy by pharmacological amelioration of glomerular capillary hypertension. *J Clin Invest* 77: 1925–1930, 1986
9. Anderson S, Rennke HG, Brenner BM: Therapeutic advantage of converting enzyme inhibitors in arresting progressive renal disease associated with systemic hypertension in the rat. *J Clin Invest* 77: 1993–2000, 1986
10. Remuzzi A, Puntorieri S, Battaglia C, Bertani T, Remuzzi G: Angiotensin converting enzyme inhibition ameliorates glomerular filtration of macromolecules and water and lessens glomerular injury in the rat. *J Clin Invest* 85: 541–549, 1990
11. Hommel E, Parving HH, Mathiesen E, Edsberg B, Damkjær M, Giese J: Effect of captopril on kidney function in insulin-dependent diabetic patients with nephropathy. *Br Med J* 293: 467–470, 1986
12. Parving HH, Hommel E, Smidt UM: Protection of kidney function and decrease in albuminuria by captopril in insulin dependent diabetics with nephropathy. *Br Med J* 297: 1086–1091, 1988
13. Bjorck S, Nyberg G, Mulec H, Granerus G, Herlitz H, Aurell M: Beneficial effects of angiotensin converting enzyme inhibition on renal function in patients with diabetic nephropathy. *Br Med J* 293: 471–474, 1986
14. Marre M, Le Blanc H, Suarez L: Converting enzyme inhibition and kidney function in normotensive diabetic patients with persistent microalbuminuria. *Br Med J* 294: 1448–1452, 1987
15. The GISEN Group: Randomised placebo-controlled trial of effect of ramipril on decline in glomerular filtration rate and risk of terminal renal failure in proteinuric, non-diabetic nephropathy. *Lancet* 349: 1857–1863, 1997
16. Yoshioka T, Rennke HG, Salant DJ, Deen WM, Ichikawa I: Role of abnormally high transmural pressure in the permselectivity

defect of glomerular capillary wall: A study in early passive Heymann nephritis. *Circ Res* 61: 531–538, 1987
17. Halbach GR, Alt JM, Brunkhorst R, Frei U, Kuhn K, Stolte H: Single nephron hyperfiltration and proteinuria in a newly selected rat strain with superficial glomeruli. *Ren Physiol* 9: 317–325, 1986
18. Remuzzi A, Puntorieri S, Alfano M, Macconi D, Abbate M, Bertani T, Remuzzi G: Pathophysiologic implications of proteinuria in a rat model of progressive glomerular injury. *Lab Invest* 67: 572–579, 1992
19. Remuzzi A, Malanchini B, Battaglia C, Bertani T, Remuzzi G: Comparison of the effects of angiotensin-converting enzyme inhibition and angiotensin II receptor blockade on the evolution of spontaneous glomerular injury in male MWF/Ztm rats. *Exp Nephrol* 4: 19–25, 1996
20. Heeg JE, de Jong PE, van der Hem GK, de Zeeuw D: Reduction of proteinuria by angiotensin converting enzyme inhibition. *Kidney Int* 32: 78–83, 1987
21. Morelli E, Loon N, Meyer TW, Peters W, Myers BD: Effects of converting-enzyme inhibition on barrier function in diabetic glomerulopathy. *Diabetes* 39: 76–82, 1990
22. Remuzzi A, Perticucci E, Ruggenenti P, Mosconi L, Limonta M, Remuzzi G: Angiotensin converting enzyme inhibition improves glomerular size-selectivity in IgA nephropathy. *Kidney Int* 39: 1267–1273, 1991
23. Ene-Iordache B, Imberti O, Foglieni C, Remuzzi G, Bertani T, Remuzzi A: Effects of angiotensin-converting enzyme inhibition on glomerular capillary wall ultrastructure in MWF/Ztm rats. *J Am Soc Nephrol* 5: 1378–1384, 1994
24. Farquhar MG: The glomerular basement membrane: A selective macromolecular filter. In: *Cell Biology of Extracellular Matrix*, edited by Hay ED, New York, Plenum Press, 1981, pp 335–378
25. Fujigaki Y, Nagase M, Kobayasi S, Hidaka S, Shimomura M, Hishida A: Intra-GBM site of the functional filtration barrier for endogenous proteins in rats. *Kidney Int* 43: 567–574, 1993
26. Robinson GB, Walton HA: Glomerular basement membrane as a compressible ultrafilter. *Microvasc Res* 38: 36–48, 1989
27. Daniels BS, Hauser EB, Deen WM, Hostetter TH: Glomerular basement membrane: In vitro studies of water and protein permeability. *Am J Physiol* 262: F919–F926, 1992
28. Daniels BS: Increased albumin permeability in vitro following alterations of glomerular charge is mediated by the cells of the filtration barrier. *J Lab Clin Med* 124: 224–230, 1994
29. Daniels BS: The role of the glomerular epithelial cell in the maintenance of the glomerular filtration barrier. *Am J Nephrol* 13: 318–323, 1993
30. Rennke HG: How does glomerular epithelial cell injury contribute to progressive glomerular damage? *Kidney Int* 45: S58–S63, 1994
31. Laurens W, Battaglia C, Foglieni C, De Vos R, Malanchini B, Van Damme B, Vanrenterghem Y, Remuzzi G, Remuzzi A: Direct podocyte damage in the single nephron leads to albuminuria in vivo. *Kidney Int* 47: 1078–1086, 1995
32. Blantz RC, Gabbai FB, Peterson O, Wilson CB, Kihara I, Kawachi H, Shimizu F, Yamamoto T: Water and protein permeability is regulated by the glomerular epithelial slit diaphragm. *J Am Soc Nephrol* 4: 1957–1964, 1994
33. Kurihara H, Anderson JM, Kerjaschki D, Farquhar MG: The altered glomerular filtration slits seen in puromycin aminonucleoside nephrosis and protamine sulfate-treated rats contain the tight junction protein ZO-1. *Am J Pathol* 141: 805–816, 1992
34. Ligler FS, Robinson GB, Byrne J: A new method for the isolation of renal basement membranes. *Biochim Biophys Acta* 468: 327–340, 1977
35. Read SM, Northcote DH: Minimization of variations in the response to different proteins of the Coomassie blue G dye-binding assay for protein. *Anal Biochem* 116: 53–64, 1981
36. McLean IW, Nakane PF: Periodate-lysine paraformaldehyde fixative: A new fixative for immunoelectron microscopy. *J Histochem Cytochem* 22: 1077–1083, 1974
37. Tokuyasu K: Immunocytochemistry on ultrathin frozen sections. *Histochem J* 12: 381–403, 1980
38. Laemnli UK: Cleavage of structural proteins during the assembly of the head of bacteriophage T4. *Nature* 227: 680–685, 1970
39. Towbin H, Staehelin T, Gordon J: Electrophoretic transfer of proteins from polyacrylamide gels to nitrocellulose sheets: Procedure and some applications. *Proc Natl Acad Sci USA* 76: 4350–4354, 1979
40. Pagtalunan ME, Rasch R, Rennke HG, Meyer TW: Morphometric analysis of effects of angiotensin II on glomerular structure in rats. *Am J Physiol* 268: F82–F88, 1995
41. Seefeldt T, Bohman S-O, Gundersen HJG, Maunsbach AB, Petersen VP, Olsen S: Quantitative relationship between glomerular foot process width and proteinuria in glomerulonephritis. *Lab Invest* 44: 541–546, 1981
42. Wallenstein S, Zucker CL, Fleiss JL: Some statistical methods useful in circulation research. *Circ Res* 47: 1–9, 1980
43. Fitzgibbon WR, Webster SK, Imamura A, Ploth DW, Hutchison FN: Effect of dietary protein and enalapril on proximal tubular delivery and absorption of albumin in nephrotic rats. *Am J Physiol* 260: F986–F996, 1996
44. Remuzzi A, Remuzzi G: Glomerular perm-selective function. *Kidney Int* 45: 398–402, 1994
45. Remuzzi A, Imberti O, Puntorieri S, Malanchini B, Macconi D, Magrini L, Bertani T, Remuzzi G: Dissociation between antiproteinuric and antihypertensive effect of angiotensin converting enzyme inhibitors in the rat. *Am J Physiol* 267: F1034–F1044, 1994
46. Robinson GB, Walton HA: Ultrafiltration through basement membrane. In: *Renal Basement Membranes in Health and Diseases*, edited by Price RG, Hudson BG, New York, London, Academic Press, 1987, pp 147–161
47. Bolton GR, Deen WM, Daniels BS: Assessment of the charge selectivity of glomerular basement membrane using Ficoll sulfate. *Am J Physiol* 274: F889–F896, 1998
48. Schnabel E, Anderson JM, Farquhar MG: The tight junction protein ZO-1 is concentrated along slit diaphragms of the glomerular epithelium. *J Cell Biol* 111: 1255–1263, 1990
49. Kurihara H, Anderson JM, Farquhar MG: Diversity among tight junctions in rat kidney: Glomerular slit diaphragms and endothelial junctions express only one isoform of the tight junction protein ZO-1. *Proc Natl Acad Sci USA* 89: 7075–7079, 1992
50. Anderson JM, Van Itallie CM: Tight junctions and the molecular basis for regulation of paracellular permeability. *Am J Physiol* 269: G467–G475, 1995
51. Kawachi H, Kurihara H, Topham PS, Brown D, Shia MA, Orikasa M, Shimizu F, Salant DJ: Slit diaphragm-reactive nephritogenic MAb 5-1-6 alters expression of ZO-1 in rat podocytes. *Am J Physiol* 273: F984–F993, 1997
52. Fujiwara Y, Kitamura E, Ueda N, Fukunaga M, Orita Y, Kamada T: Mechanism of action of angiotensin II on isolated rat glomeruli. *Kidney Int* 36: 985–991, 1989
53. Yoshioka T, Ichikawa A, Fogo A: Reactive oxygen metabolites causes massive, reversible proteinuria and glomerular sieving

defect without apparent ultrastructural abnormality. *J Am Soc Nephrol* 2: 902–912, 1991
54. Coers W, Vos JTWM, Van Der Meide PH, Van Der Horst MLC, Huitema S, Weening JJ: Interferon-gamma (IFN-γ) and IL-4 expressed during mercury-induced membranous nephropathy are toxic for cultured podocytes. *Clin Exp Immunol* 102: 297–307, 1995
55. Staddon JM, Herrenknecht K, Smales C, Rubin LL: Evidence that tyrosine phosphorylation may increase tight junction permeability. *J Cell Sci* 108: 609–619, 1995
56. Collares-Buzato CB, Jepson MA, Simmons NL, Hirst BH: Increased tyrosine phosphorylation causes redistribution of adherens junction and tight junction proteins and perturbs paracellular barrier function in MDCK epithelia. *Eur J Cell Biol* 76: 85–92, 1998
57. Kurihara H, Anderson JM, Farquhar MG: Increased tyr phosphorylation of ZO-1 during modification of tight junctions between glomerular foot processes. *Am J Physiol* 268: F514–F524, 1995
58. Leduc I, Meloche S: Angiotensin II stimulates tyrosine phosphorylation of the focal adhesion-associated protein paxillin in aortic smooth muscle cells. *J Biol Chem* 270: 4401–4404, 1995
59. Marrero MB, Schieffer B, Ma H, Bernstein KE, Ling BN: ANG II-induced tyrosine phosphorylation stimulates phospholipase C-γ1 and Cl^- channels in mesangial cells. *Am J Physiol* 270: C1834–C1842, 1996